Proceedings of the Seventh International Conference on
Railway Technology: Research, Development and Maintenance
Edited by: J. Pombo
Civil-Comp Conferences, Volume 15, Paper 11.17
Civil-Comp Press, Edinburgh, United Kingdom, 2026
ISSN: 2753-3239, doi: 10.4203/ccc.15.11.17

Superconducting Electromagnetic Suspension Train Electromagnetic Force Calculation Model Based on BP Neural Network

J. Xu[1,2], J. Xu[1,2], H. Huang[1,2], D. Gao[1,2], M. Wang[3] and W. Wu[3]

[1]College of Transportation, Tongji University, Shanghai, China
[2]State Key Lab of High Speed Maglev Transport Technology, Tongji University, Shanghai, China
[3]China Railway Design Group Co., Ltd, China

Abstract

In order to improve the calculation efficiency of electromagnetic force of superconducting electrodynamic suspension train, a fast calculation model of electromagnetic force based on BP neural network is proposed. The model takes the relative displacement between the vehicle superconducting coil and the ground suspension guide coil as the input, and the three-way mutual inductance partial derivative as the output. The mutual inductance partial derivative predicted by the neural network is substituted into the dynamic circuit equation to solve the induced current and calculate the three-way electromagnetic force. Through the simulation analysis of the electromagnetic force of the single suspension frame at different speeds, the results show that the method can improve the calculation efficiency while ensuring the calculation accuracy, and can provide an effective calculation method for the rapid simulation of the dynamics of the superconducting electrodynamic suspension train.

Keywords: superconducting electrodynamic suspension, neural network, discrete Neumann formula, dynamic circuit, electromagnetic force calculation, mutual inductance partial derivative.

1 Introduction

A superconducting electrodynamic suspension (EDS) train has the advantages of a large levitation gap, non-contact operation, and strong self-stability. Its operating speed can reach 600 km/h, making it an important research direction of high-speed maglev transportation [1-3]. The EDS maglev train generates electromagnetic forces through the relative motion between the on-board superconducting coil and the track coil to achieve stable traction, levitation, and guidance of the vehicle [4-5]. In other words, the electromagnetic coupling between the track coil and the on-board magnet in the superconducting electrodynamic suspension maglev system affects the dynamic response of the vehicle. Therefore, establishing a high-precision and high-efficiency electromagnetic force calculation model is essential for train dynamic simulation.

Extensive studies have been conducted on the modeling of electromagnetic characteristics and electromagnetic force calculation for superconducting EDS maglev systems. The main calculation methods include the finite element method and analytical methods. The finite element method can account for the three-dimensional geometric structure and material properties of the coil, and provides high computational accuracy. Chen established a finite element model capable of simulating the movement process of superconducting electrodynamic suspension maglev train, and analyzed the electromagnetic characteristics of the system [6]. Huang investigated the research on three-dimensional transient finite element modeling of superconducting electrodynamic suspension maglev train, avoided mesh deformation and reconstruction using a mapping method, and analyzed the electromagnetic characteristics at different speeds [7]. Gong established a three-dimensional finite element model of a superconducting EDS train with cross-connected figure-eight-shaped suspension coils, and studied the variation characteristics of electromagnetic force [8]. However, computational speed of the finite element method is relatively low. When it is used for long-term simulation of vehicle dynamics, its computational efficiency is insufficient for fast simulation. Compared with the finite element method, analytical methods offer higher computational speed and can more clearly reveal the electromagnetic coupling mechanism of the system. Carbonari established a three-dimensional analytical model of the EDS maglev transportation system to calculate levitation force, drag force, and lateral force [9]. Andriollo further studied the three-dimensional analytical model of the propulsion system with superconducting coils, and achieved analytical calculation of the propulsion force [10]. Cai proposed a semi-analytical calculation method for superconducting electrodynamic suspension train with 8-shaped rail coil, which is used to analyze the electromagnetic characteristics of the system [11]. Based on reasonable assumptions, Song established an analytical model of the electromagnetic force of the zero-flux coil superconducting electrodynamic suspension system, and verified the accuracy of the model using the MLX01 data of the Japanese Yamanashi test line and a small rotating test platform [12]. Huang established a semi-analytical electromagnetic model of the superconducting electrodynamic suspension system based on the Fourier series, and calculated the stiffness characteristics and suspension force fluctuations of the suspension frame [13]. Most of the above methods are based on the equivalent circuit method to calculate the electromagnetic coupling relationship between the vehicle-mounted superconducting magnet and the ground coil with the change of relative motion. By establishing the circuit equation including resistance, inductance and electromotive force, the induced current in the ground coil is solved, and then the electromagnetic force acting on the vehicle-mounted superconducting magnet is calculated by combining the virtual displacement method, energy method or Ampere force method [14]. Based on dynamic circuit theory, He established a mathematical model suitable for EDS structures such as ring coils, 8-shaped zero-flux coils, and continuous conductive plates. The model can be used for transient and dynamic performance analysis of three-dimensional electric suspension systems [15-16]. Based on the dynamic circuit theory, Hu studied the influence of superconducting EDS system parameters on levitation force, guidance force, and drag force, and verified the validity of the analytical model using a three-dimensional finite element method [17]. Tan modeled zero-flux coil superconducting electrodynamic suspension system, established numerical and analytical calculation models, respectively, and verified the accuracy of the model through experiments [18]. In recent years, in order to improve the computational efficiency of the electromagnetic force of the superconducting electrodynamic suspension maglev system, the neural network methods have gradually been introduced into the vehicle - track electromagnetic coupling modeling. Su established an analytical model of vehicle-rail electromagnetic coupling for the integrated coil system of propulsion levitation and guidance, and used a BP neural network to fit the mapping relationship between the spatial attitude of the magnet unit and the electromagnetic force, thereby improving computational efficiency [19]. Liu proposed a fast modeling method for superconducting EDS trains based on a physics-informed neural network (PINN). The dynamic circuit equation is embedded into the neural network as a physical constraint to quickly solve the induced current in the levitation guide coil, thereby realizing fast calculation of electromagnetic force [20].

In summary, existing electromagnetic force calculation methods for superconducting EDS maglev systems have formed a relatively complete framework. The finite element method can accurately describe the geometric structure and electromagnetic field distribution of the coil, and it provides high computational accuracy but low computational efficiency, making it difficult to meet the requirements of long-term dynamic simulation. The analytical method can better reveal the electromagnetic coupling mechanism of the system, and the calculation efficiency is relatively high. However, in multi-coil, long-distance, and long-term dynamic simulations, it is still necessary to repeatedly calculate the mutual inductance and partial derivative between the vehicle superconducting magnet and the ground suspension guiding coil, and the computational cost is high. The existing fast modeling neural-network-based methods mainly focus on establishing the direct mapping relationship between the magnet position and attitude and the electromagnetic force or quickly solving the induced current in the dynamic circuit equation. To address the low efficiency of repeatedly calculating the partial derivatives of mutual inductance of repeated calculation of mutual inductance partial derivative in the electromagnetic force calculation model based on dynamic circuit theory and discrete Neumann formula (DNF), a fast calculation model of electromagnetic force of superconducting electrodynamic suspension maglev based on a BP neural network is proposed in this paper. The model uses a BP neural network to predict the partial derivative of mutual inductance between coils, and substitutes them into the dynamic circuit equation to solve the induced current, so as to quickly calculate the electromagnetic force. While retaining the physical calculation process of the dynamic circuit, the model improves the calculation efficiency of the partial derivative of mutual inductance, which can provide a new approach for the rapid simulation of superconducting electrodynamic suspension maglev train dynamics.

2 EDS Suspension System Model

2.1 Dynamic Circuit Model of the Multi-Coil EDS System

The suspension-guidance system of a superconducting EDS maglev train consists of multiple groups of cross-connected figure-eight-shaped ground coils arranged periodically along the longitudinal direction. During train operation, the onboard superconducting magnets pass through these coil groups successively. Therefore, this paper directly establishes a dynamic circuit model for n groups of suspension-guidance coils. The structure and equivalent circuit of the multi-coil suspension-guidance system are shown in Figure 1, and its loop-voltage matrix equation is expressed as Equation (1).

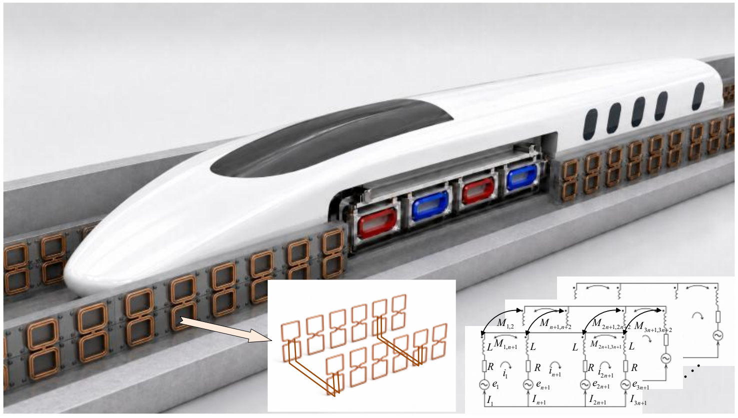

Figure 1: Structure and equivalent circuit of the multi-coil suspension-guidance system.

$$\begin{bmatrix} \boldsymbol{R}_{11} & \boldsymbol{R}_{12} & 0 \\ \boldsymbol{R}_{21} & \boldsymbol{R}_{22} & \boldsymbol{R}_{23} \\ 0 & \boldsymbol{R}_{32} & \boldsymbol{R}_{33} \end{bmatrix} \begin{bmatrix} \boldsymbol{I}_1 \\ \boldsymbol{I}_2 \\ \boldsymbol{I}_3 \end{bmatrix} + \begin{bmatrix} \boldsymbol{M}_{11} & \boldsymbol{M}_{12} & 0 \\ \boldsymbol{M}_{21} & \boldsymbol{M}_{22} & \boldsymbol{M}_{23} \\ 0 & \boldsymbol{M}_{32} & \boldsymbol{M}_{33} \end{bmatrix} \begin{bmatrix} \dfrac{\boldsymbol{dI}_1}{\boldsymbol{dt}} \\ \dfrac{\boldsymbol{dI}_2}{\boldsymbol{dt}} \\ \dfrac{\boldsymbol{dI}_3}{\boldsymbol{dt}} \end{bmatrix} = \begin{bmatrix} \boldsymbol{E}_1 \\ \boldsymbol{E}_2 \\ \boldsymbol{E}_3 \end{bmatrix} \tag{1}$$

The resistance matrix in Equation (1) is shown in Equations (2) and (3), and the submatrices of the mutual inductance matrix are all $n \times n$ matrices, as shown in Equations (4)-(6). In the mutual inductance matrix, $\boldsymbol{M}_{p,q}$ and $\boldsymbol{M}_{p,q+n}$ denote the mutual inductances of the p-th loop and the q-th or (q+n)-th loop of the coil, respectively. When only the self-inductance L of the coil loop and the mutual inductance M_{LG} of the upper and lower loops of the figure-eight-shaped coil are considered, and the mutual inductance with the adjacent position suspension guide coil loop is not considered, and are the $n \times n$ diagonal matrices with diagonal elements L and M_{LG}, respectively.

$$\boldsymbol{R}_{11} = \boldsymbol{R}_{22} = \boldsymbol{R}_{33} = \begin{bmatrix} 2R & 0 & \cdots & 0 \\ 0 & 2R & \cdots & 0 \\ \vdots & \cdots & \ddots & 0 \\ 0 & \cdots & 0 & 2R \end{bmatrix} \tag{2}$$

$$\boldsymbol{R}_{21} = \boldsymbol{R}_{32} = \boldsymbol{R}_{12} = \boldsymbol{R}_{23} = \begin{bmatrix} -R & 0 & \cdots & 0 \\ 0 & -R & \cdots & 0 \\ \vdots & \cdots & \ddots & 0 \\ 0 & \cdots & 0 & -R \end{bmatrix} \tag{3}$$

$$\boldsymbol{M}_{11}(p,q) = \boldsymbol{M}_{33}(p,q) = 2\left(\boldsymbol{M}_{p,q} - \boldsymbol{M}_{p,n+q}\right) \tag{4}$$

$$\boldsymbol{M}_{22}(p,q) = 2\boldsymbol{M}_{p,q} \tag{5}$$

$$\boldsymbol{M}_{12}(p,q) = \boldsymbol{M}_{21}(p,q) = \boldsymbol{M}_{23}(p,q) = \boldsymbol{M}_{32}(p,q) = -\boldsymbol{M}_{p,q} + \boldsymbol{M}_{p,q+n} \tag{6}$$

In this case, the loop electromotive force is shown in Equation (7). The electromotive force and loop current in the Equation (7) are shown in the Equations (8) and (9). After the loop currents are calculated, the currents in the upper and lower loops of each suspension guide coil can be obtained, and then the electromagnetic force of the *i*-th onboard magnet of the suspension frame can be obtained as shown in Equation (10).

$$\begin{bmatrix} \boldsymbol{E}_1^{\mathrm{T}} \\ \boldsymbol{E}_2^{\mathrm{T}} \\ \boldsymbol{E}_3^{\mathrm{T}} \end{bmatrix} = \begin{bmatrix} e_1 - e_{n+1} & e_2 - e_{2n+2} & \cdots & e_n - e_{2n} \\ e_{n+1} - e_{2n+1} & e_{n+2} - e_{2n+2} & \cdots & e_{2n} - e_{3n} \\ e_{2n+1} - e_{3n+1} & e_{2n+2} - e_{3n+2} & \cdots & e_{3n} - e_{4n} \end{bmatrix} \tag{7}$$

$$e_j = -\sum_{i=1}^{8} I_{\mathrm{S}}^i \left(v_x \frac{\partial M_{\mathrm{S,LG}}^{(i,j)}}{\partial x} + v_y \frac{\partial M_{\mathrm{S,LG}}^{(i,j)}}{\partial y} + v_z \frac{\partial M_{\mathrm{S,LG}}^{(i,j)}}{\partial z}\right) \tag{8}$$

$$\begin{bmatrix} \boldsymbol{I}_1^{\mathrm{T}} \\ \boldsymbol{I}_2^{\mathrm{T}} \\ \boldsymbol{I}_3^{\mathrm{T}} \end{bmatrix} = \begin{bmatrix} i_1 & i_2 & \cdots & i_n \\ i_{n+1} & i_{n+2} & \cdots & i_{2n} \\ i_{2n+1} & i_{2n+2} & \cdots & i_{3n} \end{bmatrix} \tag{9}$$

$$\boldsymbol{F}_{\mathrm{S}}^i = -I_{\mathrm{S}}^i \sum_{j=1}^{4n} I_j \frac{\partial M_{\mathrm{S,LG}}^{(i,j)}}{\partial \boldsymbol{X}} \tag{10}$$

In Equation (10), $\boldsymbol{F}_{\mathrm{S}}^{i}=\begin{bmatrix}F_{\mathrm{S}x}^{i} & F_{\mathrm{S}y}^{i} & F_{\mathrm{S}z}^{i}\end{bmatrix}$ is the electromagnetic force in the three directions of the *i*-th onboard magnet. Based on the above formulation, a dynamic circuit model of the superconducting electrodynamic suspension multi-coil system is established. In this model, the circuit parameters, including resistance and self-inductance can be calculated according to the given coil dimensions and number of turns.

2.2 Mutual Inductance Model Between the Superconducting Magnet and the Levitation-Guidance Coil

In calculating the electromagnetic forces of onboard magnets, a large number of mutual inductance values and their partial derivatives must be calculated. In this paper, the DNF is used to calculate the mutual inductance between the superconducting coil and the suspension-guidance coil. The racetrack-shaped superconducting coil and the rectangular suspension guide coil are discretized into a finite number of straight-line segments to calculate the mutual inductance. The mutual inductance between the superconducting coil and the levitation guide coil can be written as a double line-integral form, as shown in Equation (11). In Equation (11), μ_0 is the vacuum permeability, N_{S} and N_{LG} are the turns of the superconducting coil and the levitation guide coil, respectively, $\boldsymbol{S}^{*}$ denotes the coordinates of the superconducting coil, and $\boldsymbol{LG}^{*}$ denotes the coordinates of the levitation-guidance coil.

$$M_{\mathrm{S,LG}}^{(i,j)}=\frac{\mu_0 N_{\mathrm{S}} N_{\mathrm{LG}}}{2\pi}\sum_{i_{\mathrm{s}}=1}^{n_{\mathrm{s}}}\sum_{j_{\mathrm{lg}}=1}^{n_{\mathrm{lg}}}\frac{(\boldsymbol{S}_i^{*}(i_{\mathrm{s}}+1)-\boldsymbol{S}_i^{*}(i_{\mathrm{s}}))\cdot(\boldsymbol{LG}_j^{*}(j_{\mathrm{lg}}+1)-\boldsymbol{LG}_j^{*}(j_{\mathrm{lg}}))}{\left|\boldsymbol{S}_i^{*}(i_{\mathrm{s}}+1)+\boldsymbol{S}_i^{*}(i_{\mathrm{s}})-(\boldsymbol{LG}_j^{*}(j_{\mathrm{lg}}+1)+\boldsymbol{LG}_j^{*}(j_{\mathrm{lg}}))\right|} \tag{11}$$

2.3 Electromagnetic Force Calculation Model Based on a BP Neural Network

BP neural network is a kind of feedforward neural network based on error back propagation algorithm training, which can approximate complex function relationship through multi-layer nonlinear mapping. Its structure is shown in Figure 2. In this paper, the neural network is used instead of DNF to calculate the partial derivative of mutual inductance. The neural network parameters used are as shown in table 1, and the hidden layer is fully connected. The input of the neural network is the relative displacement of the superconducting coil to the levitation guide coil, that is $\mathbf{X}=\begin{bmatrix}x & y & z\end{bmatrix}$. The output of the neural network is the mutual inductance partial derivative of the superconducting coil to the three directions of the four levitation guide coils, that is $\mathbf{Y}=\begin{bmatrix}\frac{\partial M}{\partial x_j} & \frac{\partial M}{\partial y_j} & \frac{\partial M}{\partial z_j}\end{bmatrix}$. $\frac{\partial M}{\partial x_j}$, $\frac{\partial M}{\partial y_j}$ and $\frac{\partial M}{\partial z_j}$ represent the partial derivatives of the mutual inductance between the superconducting coil and the *j*-th levitation guide coil to the displacement in the directions of *x*, *y* and *z*, respectively. The training samples of the neural network are generated by DNF, and several sampling points are selected within a given relative displacement range. Each sampling point corresponds to the position of a superconducting coil relative to the current levitation guide coil group. According to this position, the spatial coordinates of the superconducting coil and the four levitation guide coils are constructed, and then the three-dimensional mutual inductance partial derivatives between the superconducting coil and the four levitation guide coils are calculated respectively. The input and output of the training samples are normalized before training. After the training, the network prediction value needs to be denormalized to restore to the real physical quantity, and then substituted into the dynamic circuit equation to calculate the electromagnetic force.

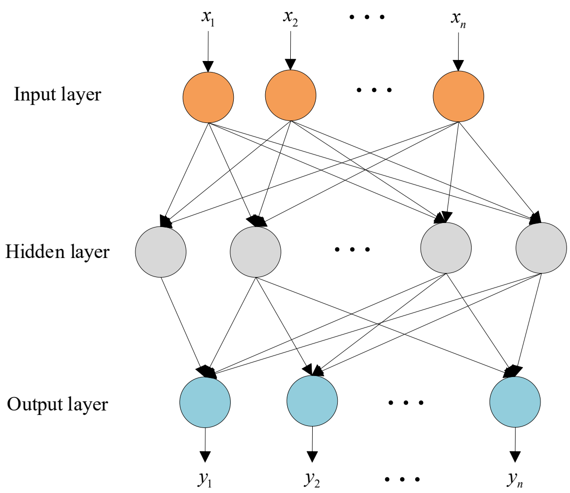

Figure 2: BP neural network structure diagram.

Parameter [-]	Value [-]
Network size [-]	[3 128 128 128 12]
Learning rate [-]	1e-4
Number of samples [-]	40000
Activation function [-]	tanh
Number of iterations [-]	30000

Table 1: BP neural network parameters.

3 Results

In order to verify the effectiveness of the proposed method, in the dynamic calculation of superconducting maglev train, the superconducting coil passes through the suspension guide coil at a uniform speed along the longitudinal direction. At each time step, the BP neural network method and DNF are used to calculate the partial derivatives of mutual inductance, and the induced current and electromagnetic force are solved under the same circuit equation. The two methods use the same geometric parameters, circuit parameters, initial current conditions, time step and motion speed. Coil geometry parameters and circuit parameters are shown in Table 2. In order to evaluate the performance of BP neural network, mean root mean square error (RMSE) and mean absolute error (MAE) are used as evaluation indexes. Assuming that the calculation result of the DNF method is y_{true}, the calculation result of the BP neural network method is y_{pred}, and the number of samples is n, the three error indicators are defined as Equations (12) and (13). The electromagnetic force during the operation of a single suspension frame is studied. A single suspension frame contains 8 superconducting coils. The longitudinal polar distance of the superconducting coil is 1350 mm. The suspension guide coils on the track are arranged longitudinally, and the polar distance is 450 mm. In the calculation of electromagnetic force, the sliding window method is used to reduce the calculation amount of the circuit differential equation. In order to verify the applicability of the fast calculation model in this paper under different speed conditions, the floating, high-speed operation and ultra-high-speed operation speed are selected, that is $v = \begin{bmatrix}150 & 300 & 500\end{bmatrix}\text{km/h}$, the electromagnetic characteristics of the suspension frame during operation are simulated and calculated. The suspension frame operates in the case of lateral offset $\Delta y = 0$ and vertical offset $\Delta z = -40\text{mm}$.

$$RMSE = \sqrt{\frac{1}{n}\sum_{i=1}^{n}(y_{itrue} - y_{ipred})^2} \tag{12}$$

$$MAE = \frac{1}{n}\sum_{i=1}^{n}\left|y_{itrue} - y_{ipred}\right| \tag{13}$$

Parameter [-]	Value [-]
Length of superconducting coil straight section [mm]	570
Curve radius of superconducting coil [mm]	250
Magnetomotive force of superconducting coil [kA]	700
Number of turns of superconducting coils [turns]	350
Height of the straight section of the levitation-guidance coil [mm]	340
Length of the straight section of the levitation-guidance coil [mm]	350

Number of turns of levitation-guidance coil [turns]	35
Mutual inductance of upper and lower loops of levitation-guidance coil [μH]	19.4
Single loop self-inductance of levitation-guidance coil [mH]	0.288
Single loop resistance of levitation-guidance coil [mΩ]	7.6

Table 2: Coil geometry parameters and circuit parameters.

3.1 Electromagnetic Force

The unilateral electromagnetic force simulation results of the suspension frame at 150, 300 and 500 km/h are shown in Figures 3-5, respectively. The figures show that the three-component electromagnetic force calculated by the two methods are generally consistent in terms of variation trend and fluctuation phase under different speed conditions, indicating that the BP neural network can accurately predict the partial derivatives of mutual inductance between the superconducting coil and the suspension guide coil, and further capture the variation of electromagnetic force with operating position. The magnetic drag force and guidance force obtained by the two methods agree well. Although the levitation force exhibits a certain amplitude difference in the steady-state stage, the overall change trend is still consistent. These results indicate that the BP neural network can replace the DNF method while ensuring that consistency in the main variation characteristics of the electromagnetic force.

3.2 Electromagnetic Force Calculation Error

The electromagnetic force calculation errors of the BP neural network method at different speeds are shown in Figure 6, where the ordinate is plotted on a logarithmic scale. The figure shows that the calculation errors of the BP neural network method are generally similar under different speed conditions. The magnetic drag force and guidance force exhibit higher calculation accuracy, whereas the levitation force shows relatively larger errors. The RMSE values of the magnetic drag force at 150, 300, and 500 km/h are 736.33, 750.48, and 759.04 N, respectively, and the corresponding MAE values are 655.99, 667.87, and 668.37 N. The guidance-force errors are relatively small, with RMSE values of 0.0042, 0.0148, and 0.0038 N and MAE values of 0.0032, 0.0121, and 0.0030 N, respectively. In contrast, the levitation-force errors are relatively large, with RMSE values of 11723, 11086, and 10623 N and MAE values of 11585, 10872, and 10331 N, respectively. Overall, the BP neural network method achieves good computational accuracy under different speed conditions.

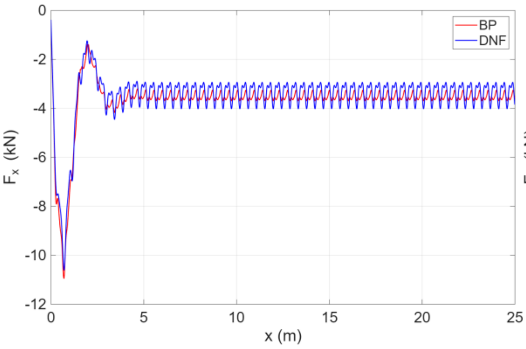

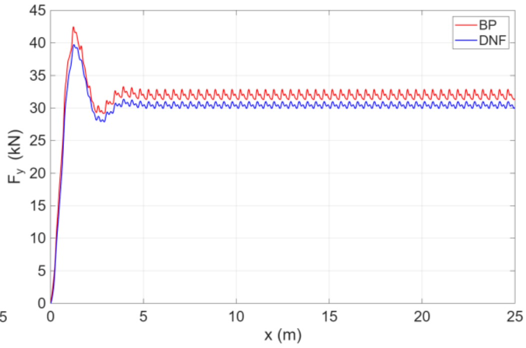

(a) Magnetic drag force (b) Guidance force

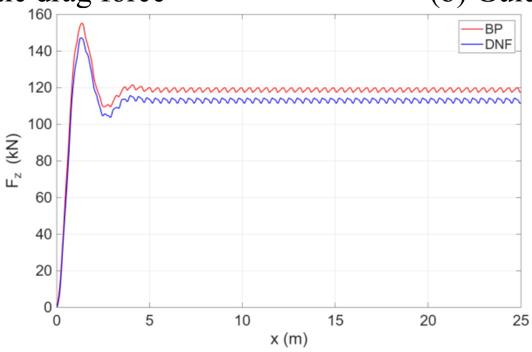

(c) Levitation force

Figure 3: Calculation results of single-side electromagnetic force at 150 km/h.

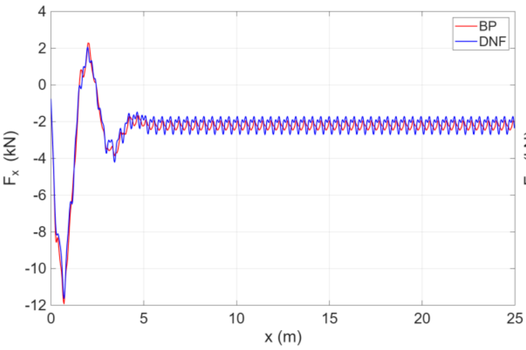

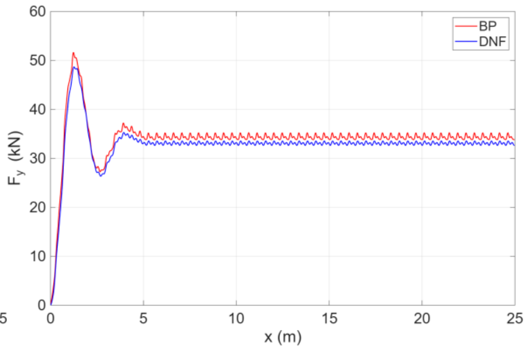

(a) Magnetic drag force (b) Guidance force

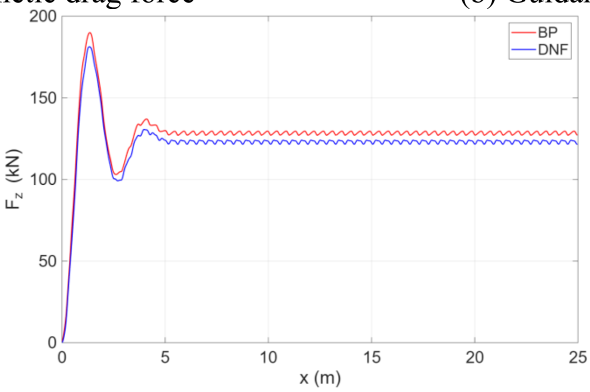

(c) Levitation force

Figure 4: Calculation results of single-side electromagnetic force at 300 km/h.

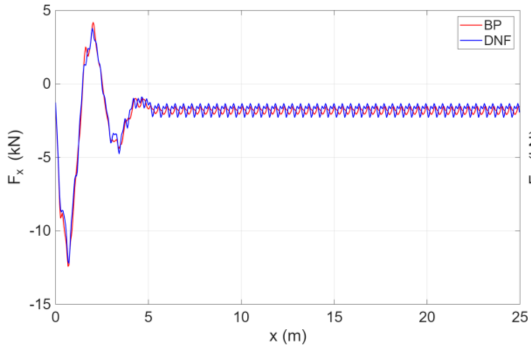

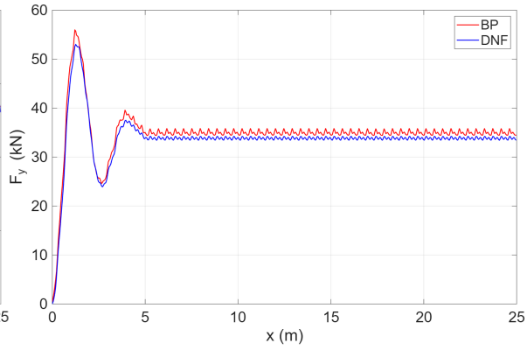

(a) Magnetic drag force (b) Guidance force

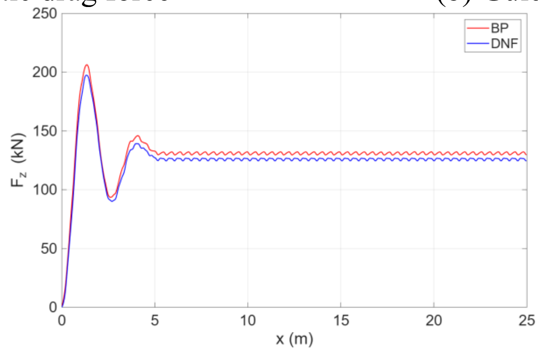

(c) Levitation force

Figure 5: Calculation results of single-side electromagnetic force at 500 km/h.

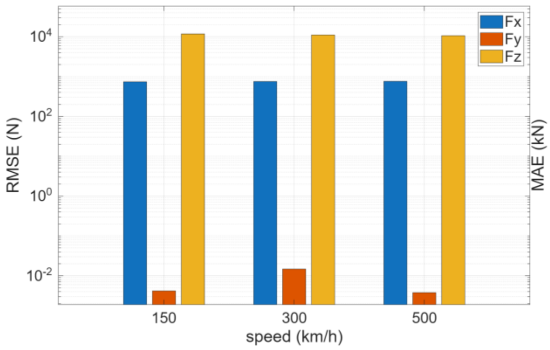

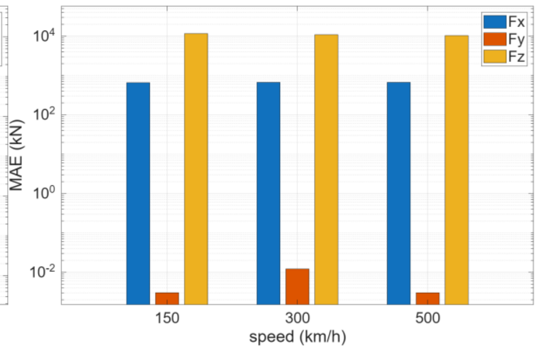

(a) RMSE (b) MAE

Figure 6: Electromagnetic force calculation errors at different speeds.

3.3 Calculation Time

The calculation times of the two methods for a 25 m run at different speeds are shown in Table 3. At 150 km/h, the calculation time of the BP neural network method is 7.50 s, whereas that of the DNF method is 37.41 s, corresponding to a reduction of approximately 79.95%. At 300 km/h, the calculation times of the two methods are 3.44 and 17.86 s, respectively, corresponding to a reduction of approximately 80.74%. At 500 km/h, the calculation times are 2.12 and 10.82 s, respectively, corresponding to a reduction of approximately 80.41%. These results show that the BP neural network method requires significantly less calculation time than the DNF method, indicating that neural-network-based prediction of the partial derivatives of mutual inductance can effectively improve the computational efficiency of electromagnetic force calculation.

Speed [km/h]	BP calculation time [s]	DNF calculation time [s]
150	7.50	37.41
300	3.44	17.86
500	2.12	10.82

Table 3: The calculation time of the two methods.

4 Conclusions and Contributions

In this paper, a fast electromagnetic force calculation model based on a BP neural network is proposed to address the low computational efficiency of numerical calculation in the calculation of electromagnetic force of superconducting EDS maglev train. In this method, the relative displacement between the superconducting coil and the suspension guide coil is used as the input, and the partial derivative of mutual inductance is used as the output. The output of the neural network is substituted into the dynamic circuit equation to solve the induced current and the three-component electromagnetic forces. Through simulations of a single suspension frame under different speed conditions, the following conclusions are obtained:

(1) The BP neural network can effectively replace the DNF method to calculate the partial derivative of mutual inductance, and can accurately approximate the variation characteristics of the partial derivative of mutual inductance, which provides a basis for the subsequent rapid calculation of electromagnetic force.

(2) Under different speed conditions, the magnetic resistance, guiding force and suspension force calculated by the BP neural network method and the DNF method are generally consistent in terms of variation trend and fluctuation phase. The BP neural network method achieves higher calculation accuracy for the magnetic drag force and guidance force, while the levitation-force calculation error is relatively large.

(3) The BP neural network method can significantly improve the efficiency of electromagnetic force calculation. At different speeds, the calculation time of the neural network method is significantly lower than that of the DNF method, and the calculation time is reduced by approximately 80%.

Since the dynamic simulation of the superconducting electrodynamic suspension train requires repeated calculations of the mutual inductance partial derivative between the superconducting coil and the suspension guide coil over a large number of time steps, this method can provide a new approach for the rapid calculation of the dynamics of the superconducting electrodynamic suspension train.

Acknowledgements

This work was supported in part by the National Natural Science Foundation of China (52232013, 52502448) and Basic Research Fund for Central Universities (22120230311).

References

[1] J. R. Powell and G. T. Danby, "Magnetic suspension for levitated tracked vehicles", Cryogenics, 11(3), 192-204, 1971.
[2] K. Sawada, "Outlook of the superconducting Maglev", Proceedings of the IEEE, 97(11), 1881-1885, 2009.
[3] H. Huang, H. Li, C. Tim, et al, "Advancements in dynamic characteristics analysis of superconducting electrodynamic suspension systems: Modeling, experiment and optimization", Superconductivity, 11, 100114, 2024.
[4] L. Beauloye and B. Dehez, "Permanent Magnet Electrodynamic Suspensions Applied to MAGLEV Transportation Systems: A Review", IEEE Transactions on Transportation Electrification, 9(1), 748-758, 2023.
[5] S. Liu, L. Wang, L. Wang, et al, "Review on Electrodynamic Suspension Trains and on-Board Superconducting Magnets", JOURNAL OF SOUTHWEST JIAOTONG UNIVERSITY, 58(4), 734-753, 2023.
[6] D. Chen, X. Li, X. Huang, et al, "An FEM Model for Evaluation of Force Performance of High-Temperature Superconducting Null-Flux Electrodynamic Maglev System", IEEE Transactions on Applied Superconductivity, 31(7), 1-6, 2021.
[7] H. Huang, Z. Deng, H. Li, et al, "Numerical Simulation of Dynamic Electromagnetic Characteristics of Superconducting Electrodynamic Suspension (EDS) Train", IEEE Transactions on Applied Superconductivity, 31(5), 1-5, 2021.
[8] T. Gong, G. Ma, R. Wang, et al, "3-D FEM Modeling of the Superconducting EDS Train With Cross-Connected Figure-Eight-Shaped Suspension Coils", IEEE Transactions on Applied Superconductivity, 31(3), 1-13, 2021.
[9] N. Carbonari, G. Martinelli and A. Morini, "Calculation of levitation, drag and lateral forces in EDS-MAGLEV transport systems", Archiv für Elektrotechnik, 71, 139-148, 1988.
[10] M. Andriollo, G. Martinelli, M. F. Moisio, et al, "Calculation of propulsion forces in EDS-MAGLEV transport systems with superconducting coils", Archiv für Elektrotechnik, 72, 333-339, 1989.
[11] Y. Cai, G. Ma, Y. Wang, et al, "Semianalytical Calculation of Superconducting Electrodynamic Suspension Train Using Figure-Eight-Shaped Ground Coil", IEEE Transactions on Applied Superconductivity, 30(5), 1-9, 2020.
[12] M. Song, D. Zhou, P. Yu, et al, "Analytical Calculation and Experimental Verification of Superconducting Electrodynamic Suspension System Using Null-Flux Ground Coils", IEEE Transactions on Intelligent Transportation Systems, 23(9), 14978-14989, 2022.

[13] H. Huang, H. Li, H. Zhu, et al, "Semi-analytical Electromagnetic Model and Stiffness Characteristics of Superconducting Electrodynamic Suspension Based on the Fourier Series Method", JOURNAL OF MECHANICAL ENGINEERING, 61(14), 261-272, 2025.
[14] T. N. França, H. Li, H. Zhu, et al, "Electrical Circuits Simulator in Null-Flux Electrodynamic Suspension Analysis", Applied Sciences, 13(11), 6666, 2023.
[15] J. He, D. M. Rote and H. T. Coffey, "Applications of the dynamic circuit theory to Maglev suspension systems", IEEE Transactions on Magnetics, 29(6), 4153-4164, 1993.
[16] J. He and H. Coffey, "Magnetic damping forces in figure-eight-shaped null-flux coil suspension systems", IEEE Transactions on Magnetics, 33(5), 4230-4232, 1997.
[17] D. Hu and M. Zhai, "Study on the characteristics of superconducting electrodynamic suspension system based on dynamic circuit theory", COMPEL, 40(1), 62-73, 2021.
[18] Y. Tan, D. Zhou, Q. Chen, et al, "Research on the Calculation Methods of the Mathematical Model of Null-Flux Coil Electrodynamic Suspension System and Experimental Verification", IEEE Transactions on Transportation Electrification, 11(1), 3015-3027, 2025.
[19] Z. Su, J. Luo, P. Feng, et al, "Vertical-Lateral Coupled Dynamic Model for Integrated Propulsion, Levitation and Guidance Superconducting EDS Train", IEEE Transactions on Intelligent Transportation Systems, 25(5), 4364-4375, 2024.
[20] L. Liu, W. Dong, H. Ye, et al, "Efficiently Modeling of Superconducting Electrodynamic Suspension Train Based on Physics-informed Neural Network", IECON 2025-51st Annual Conference of the IEEE Industrial Electronics Society, Madrid, Spain, 1-7, 2025.